G$_{q/11}$α and G$_s$α mediate distinct physiological responses to central melanocortins

Yong-Qi Li,[1] Yogendra Shrestha,[1] Mritunjay Pandey,[1] Min Chen,[1] Ahmed Kablan,[1] Oksana Gavrilova,[2] Stefan Offermanns,[3] and Lee S. Weinstein[1]

[1]Metabolic Diseases Branch and [2]Mouse Metabolism Core Laboratory, National Institute of Diabetes and Digestive and Kidney Diseases (NIDDK), NIH, Bethesda, Maryland, USA.
[3]Max Planck Institute for Heart and Lung Research, Bad Nauheim, Germany.

Activation of brain melanocortin 4 receptors (MC4Rs) leads to reduced food intake, increased energy expenditure, increased insulin sensitivity, and reduced linear growth. MC4R effects on energy expenditure and glucose metabolism are primarily mediated by the G protein G$_s$α in brain regions outside of the paraventricular nucleus of the hypothalamus (PVN). However, the G protein(s) that is involved in MC4R-mediated suppression of food intake and linear growth, which are believed to be regulated primarily though action in the PVN, is unknown. Here, we show that PVN-specific loss of G$_q$α and G$_{11}$α, which stimulate PLC, leads to severe hyperphagic obesity, increased linear growth, and inactivation of the hypothalamic-pituitary-adrenal axis, without affecting energy expenditure or glucose metabolism. Moreover, we demonstrate that the ability of an MC4R agonist delivered to PVN to inhibit food intake is lost in mice lacking G$_{q/11}$α in the PVN but not in animals deficient for G$_s$α. The blood pressure response to the same MC4R agonist was only lost in animals lacking G$_s$α specifically in the PVN. Together, our results exemplify how different physiological effects of GPCRs may be mediated by different G proteins and identify a pathway for appetite regulation that could be selectively targeted by G$_{q/11}$α-biased MC4R agonists as a potential treatment for obesity.

Introduction

Obesity is an ever-increasing public health problem, leading to a significantly increased risk of many disorders, including diabetes and cardiovascular disease. Melanocortins within the CNS activate the G protein–coupled melanocortin 4 receptor (MC4R), leading to negative energy balance (reduced food intake, increased sympathetic nerve activity, and energy expenditure) and increased insulin sensitivity as well as effects on linear growth and cardiovascular function. Inactivating MC4R mutations are the most common cause of human monogenic obesity and lead to several distinct physiological effects, including increased adiposity, body length, and food intake and reduced energy expenditure and peripheral insulin sensitivity (1–3). Reexpression of MC4R in the paraventricular nucleus of the hypothalamus (PVN) of MC4R KO (*Mc4r*$^{-/-}$) mice reverses the abnormality in food intake but not in energy expenditure, indicating that in the PVN MC4R regulates food intake, while in CNS regions outside of the PVN, MC4R regulates energy expenditure (4). Single-minded homolog 1 (SIM1) is a transcription factor expressed in the PVN as well as the supraoptic nucleus and amygdala. MC4R is believed to mediate its effects on food intake and body length by inducing SIM1 expression; as the MC4R (and MC3R) agonist melanotan II (MTII) induces SIM1 expression in the PVN (5), SIM1 overexpression reverses hyperphagia associated with reduced MC4R signaling (6), and SIM1 mutations lead to hyperphagic obesity and increased linear

growth without affecting energy expenditure (5, 7). Furthermore, in SIM1 mutant mice, MTII inhibition of food intake is impaired, while MTII stimulation of energy expenditure is unaffected (5).

MC4R is known to signal through G$_s$α (encoded by *GNAS*), a ubiquitously expressed G protein that mediates receptor-stimulated cAMP production. Pseudohypoparathyroidism type 1a is a monogenic obesity disorder caused by inactivating G$_s$α mutations (8). Mice with germline or brain-specific mutation of the maternal *Gnas* allele (mBrGsKO) develop severe obesity with reduced sympathetic nerve activity and energy expenditure and early-onset insulin-resistant diabetes, with no effect on food intake or body length (9). Moreover, opposite to that in SIM1 mutant mice (5), MTII inhibition of food intake is unaffected, while MTII stimulation of energy expenditure is impaired in mBrGsKO mice (9). Mice with G$_s$α deficiency in the PVN (mPVNGsKO) showed no significant effects on food intake, energy expenditure, MTII responsiveness, or body length and no primary effects on glucose metabolism (10). It therefore appears that MC4R mediates its effects on energy expenditure and glucose metabolism via G$_s$α in CNS regions outside of the PVN, while MC4R effects on food intake and linear growth occur via a SIM1-dependent but G$_s$α-independent pathway within the PVN. The concept that G$_s$α does not mediate all of the actions of MC4R is consistent with the fact that many MC4R mutations identified in obese patients show normal activation of G$_s$α/cAMP signaling (11).

The question remains as to what mediates MC4R actions on food intake and linear growth in the PVN. Another G protein besides G$_s$α could be involved, as GPCRs are known to couple to multiple G proteins (12). G$_q$α and G$_{11}$α (encoded by *GNAQ* and
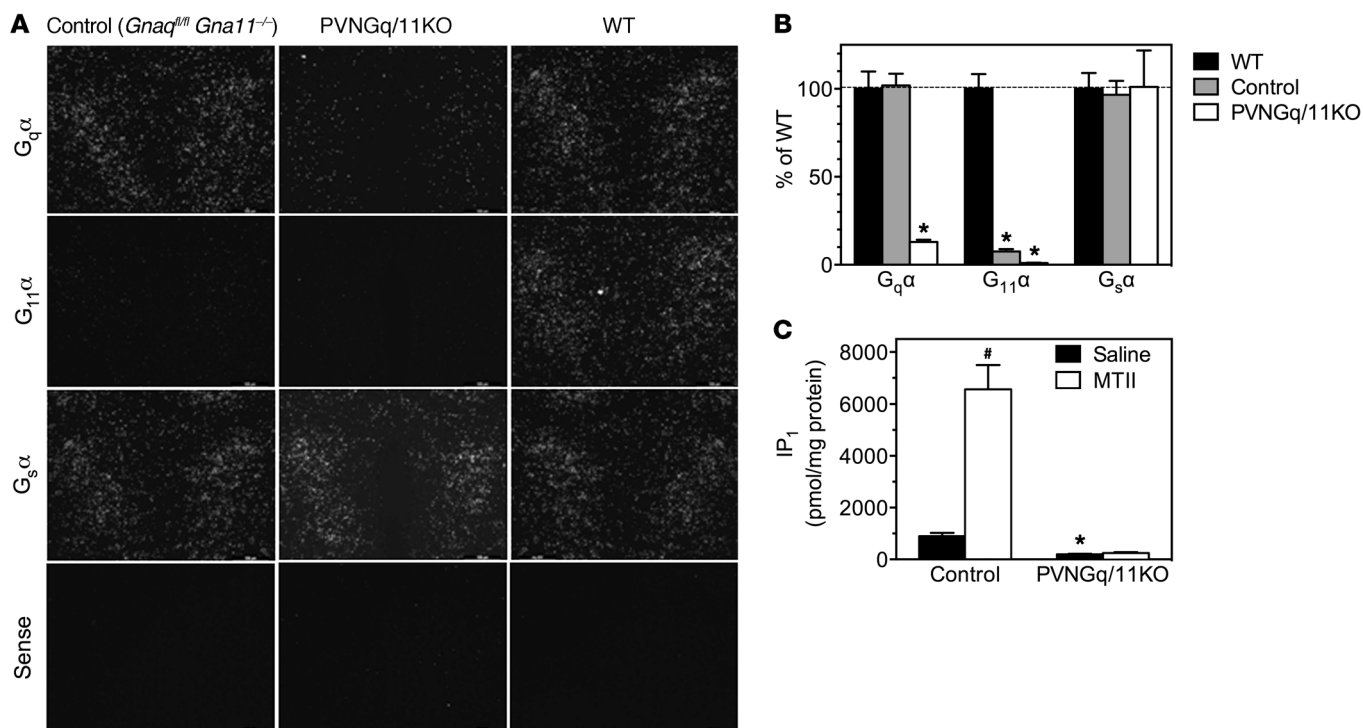
Figure 1. Loss of $G_q\alpha$ and $G_{11}\alpha$ expression in the PVNs of PVNGq/11KO mice. (**A**) In situ hybridization with antisense $G_q\alpha$-, $G_{11}\alpha$-, and $G_s\alpha$-specific probes and a sense $G_q\alpha$-specific probe in the PVNs of control (*Gnaq^{fl/fl} Gna11^{-/-}*), PVNGq/11KO, and WT mice (original magnification, ×20) (see Supplemental Table 2 for probe sequences). Hybridization with sense $G_{11}\alpha$- and $G_s\alpha$-specific probes also showed no significant signal (data not shown). (**B**) Quantitation of in situ hybridization studies, with results expressed as percentage of WT (*n* = 6 per group). Our results show that in controls expression of $G_{11}\alpha$ but not $G_q\alpha$ is lost, while in PVNGq/11KO mice expression of both $G_q\alpha$ and $G_{11}\alpha$ is lost. $G_s\alpha$ expression is unaffected in all mouse lines. *P < 0.05 by 1-way ANOVA. (**C**) IP_1 levels (normalized to protein) in PVNs from control and PVNGq/11KO mice after a 1-hour exposure to saline or MTII (50 nM) ex vivo (*n* = 6 per group). *P < 0.05 vs. control, #P < 0.05 vs. saline by Student's *t* test. Data are expressed as mean ± SEM.

GNA11, respectively) are two highly homologous ubiquitously expressed G proteins that couple receptors to PLC, resulting in stimulation. Neither $G_q\alpha$ KO (*Gnaq^{-/-}*) (13) nor $G_{11}\alpha$ KO (*Gna11^{-/-}*) (14) mice develop an obvious metabolic phenotype. MC4R signaling through $G_{q/11}\alpha$ has been documented in hypothalamic neurons (15–17), and cultured hypothalamic neurons have been documented to simultaneously generate both cAMP signals (via $G_s\alpha$) and PLC/Ca^{2+} signals (via $G_{q/11}\alpha$) (17). The dopamine D1 receptor was shown to differentially couple to $G_s\alpha$ and $G_{q/11}\alpha$ in different brain regions (18). We therefore hypothesized that $G_{q/11}\alpha$ may mediate MC4R actions on food intake and linear growth in the PVN. In this study, we provide evidence that PVN/$G_{q/11}\alpha$ pathways mediate the melanocortin effects on feeding behavior and linear growth and are also important regulators of the hypothalamic-pituitary-adrenal axis.

Results

Generation of PVNGq/11KO mice. To study the role of $G_{q/11}\alpha$ signaling in the PVN on metabolic regulation, we generated mice that lacked both $G_q\alpha$ and $G_{11}\alpha$ in the PVN (*Sim1-Cre Gnaq^{fl/fl} Gna11^{-/-}* mice, herein referred to as PVNGq/11KO mice), which was confirmed

by in situ hybridization (Figure 1, A and B). Expression of *Sim1-Cre* is relatively specific for PVN but is also expressed in the supraoptic nucleus, the amygdala, and the anterior periventricular nucleus of the hypothalamus (4). As previously reported (14), *Gnaq^{fl/fl} Gna11^{-/-}* mice were indistinguishable from WT littermates and had a normal metabolic phenotype (Supplemental Figure 1; supplemental material available online with this article; doi:10.1172/JCI76348DS1) and therefore were used as controls. The number of mutants alive at weaning was consistent with expected Mendelian ratios.

Table 1. Serum chemistries in female PVNGq/11KO and control mice in the fed state

	Young mice (6–10 weeks of age)		Old mice (24–28 weeks of age)	
	Control	PVNGq/11KO	Control	PVNGq/11KO
Glucose (mg/dl)	92 ± 5	100 ± 3	93 ± 3	117 ± 3[A]
Free fatty acids (mM)	0.50 ± 0.06	0.53 ± 0.06	0.63 ± 0.08	0.52 ± 0.06
Triglycerides (mg/dl)	119 ± 18	151 ± 23	101 ± 9	113 ± 11
Cholesterol (mg/dl)	95 ± 8	132 ± 7[A]	104 ± 8	151 ± 12[A]
Insulin (ng/ml)	0.62 ± 0.08	0.75 ± 0.12	0.61 ± 0.07	1.88 ± 0.43[A]
Leptin (ng/ml)	5.3 ± 1.3	7.8 ± 2.1	10.4 ± 1.5	37.0 ± 6.0[A]
Adiponectin (μg/ml)	13.6 ± 1.0	11.4 ± 0.9	20.7 ± 1.8	24.4 ± 4.8

Data are expressed as mean ± SEM (*n* = 7–13 per group). [A]P < 0.05 vs. controls by Student's *t* test.
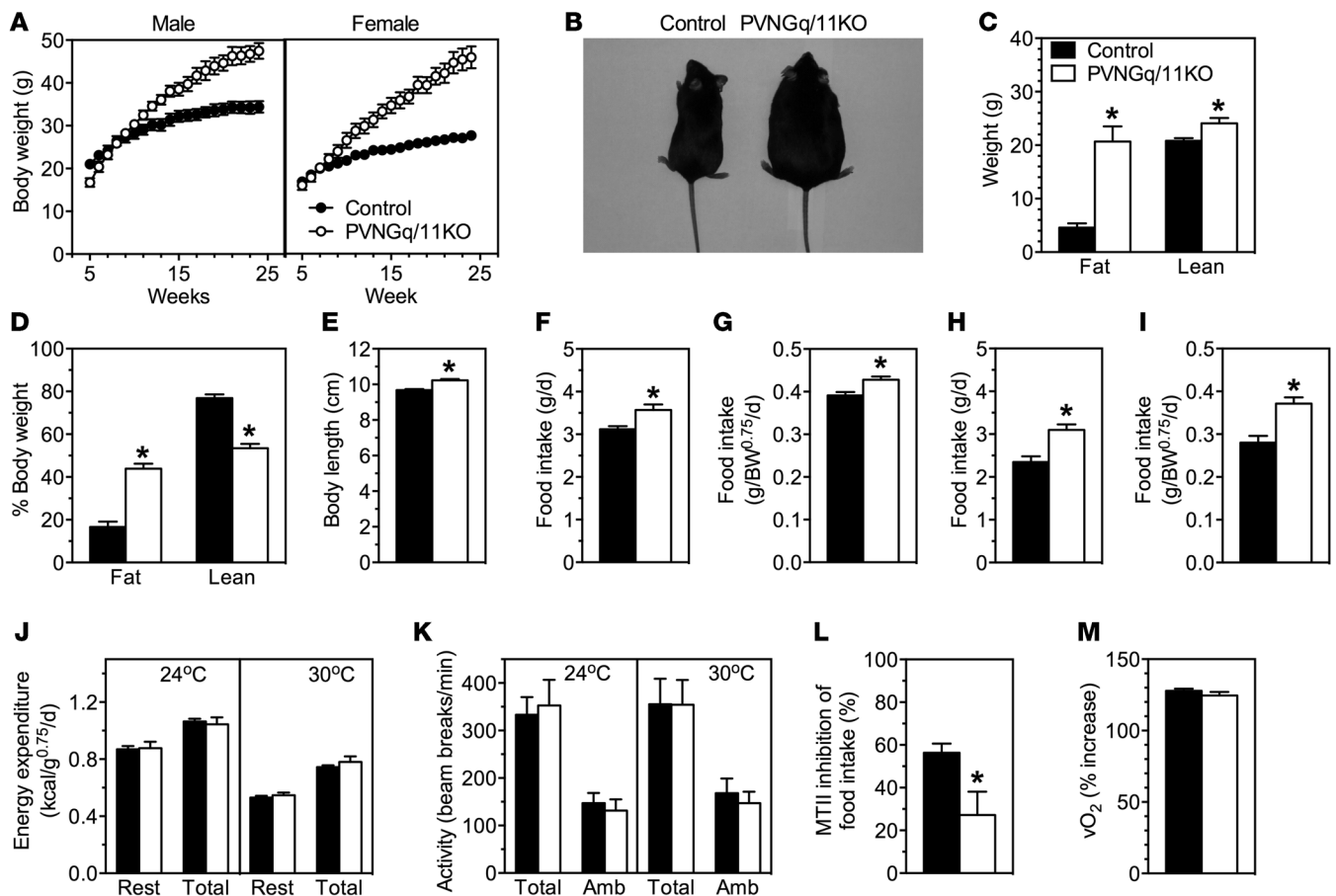
Figure 2. PVNGq/11KO mice develop hyperphagia and severe obesity. (**A**) Body weight curves of male (n = 6–7 per group) and female (n = 8–13 per group) PVNGq/11KO mice and respective controls. (**B**) Representative image of a 24-week-old female PVNGq/11KO mouse and a control mouse. (**C–E**) Body composition showing (**C**) absolute lean and fat mass, (**D**) fat and lean mass expressed as a percentage of body weight, and (**E**) body length of 24- to 28-week-old female PVNGq/11KO and control mice (n = 8–9 per group). (**F** and **H**) Absolute food intake and (**G** and **I**) food intake normalized to body weight in 6- to 8-week-old female PVNGq/11KO mice and controls measured at (**F** and **G**) 24°C and at (**H** and **I**) thermoneutrality (30°C) (n = 6–8 per group). (**J**) Resting (Rest) and TEE and (**K**) total and ambulatory (Amb) motor activity at 24°C and 30°C in 6- to 8-week-old female PVNGq/11KO and control mice (n = 8 per group). (**L**) Percentage inhibition of food intake after MTII administration, as compared to that after injection with PBS vehicle in 8- to 10-week-old female mice (n = 6–7 per group). (**M**) Percentage increase in TEE (O$_2$ utilization) at 30°C after MTII administration, as compared to that after injection with PBS in 8- to 10-week-old female mice (n = 7 per group). Data are expressed as mean ± SEM. *P < 0.05 vs. controls by Student's t test.

As PLC is the major effector of G$_q$α and G$_{11}$α, we examined the effect of knocking out these G proteins on PLC signaling in the PVN. PVNs from control and PVNGq/11KO mice were isolated and incubated with either PBS or MTII, and accumulation of inositol monophosphate (IP$_1$), a metabolite of inositol triphosphate (IP$_3$), was examined in the presence of LiCl, which inhibits the metabolism of IP$_1$ (19). Baseline IP$_1$ levels (after PBS administration) in the PVNs from PVNGq/11KO mice were only 21% of those present in controls (Figure 1C), consistent with G$_q$α and G$_{11}$α being lost in the PVN. Moreover, while MTII stimulated IP$_1$ levels 7.3-fold in the PVNs from control mice, MTII incubation had no effect on IP$_1$ levels in the PVNs from PVNGq/11KO mice (Figure 1C), indicating that a melanocortin MC3/4R agonist can stimulate G$_{q/11}$α/PLC signaling in the PVN.

PVNGq/11KO mice develop hyperphagia and obesity. PVNGq/11KO mice developed severe obesity (Figure 2, A and B), with markedly increased fat mass (Figure 2, C and D). Similar to *Mc4r*$^{-/-}$ (3) and SIM1 mutant mice (20), female mice had a greater disparity

in body weight between mutant and control mice. Consistent with increased adiposity, PVNGq/11KO mice also developed severe hyperleptinemia (Table 1). Absolute lean mass was also increased, although less strikingly than fat mass, and was decreased when expressed as a percentage of total body weight (Figure 2D). Some of the increase in lean mass was due to PVNGq/11KO mice having increased body length (Figure 2E), a characteristic associated with both MC4R (2, 3) and SIM1 (5, 7) mutations but not observed in mBrGsKO mice (9).

At 6 to 8 weeks of age, before the onset of obesity, PVNGq/11KO mice ate significantly more than controls at both room temperature (24°C; Figure 2, F and G) and at thermoneutrality (30°C, Figure 2, H and I). In contrast, there were no differences in resting energy expenditure and total energy expenditure (TEE) or activity levels between groups at either 24°C or 30°C (Figure 2, J and K). Similarly, PVNGq/11KO mice also showed hyperphagia at 12 to 16 weeks of age (Supplemental Figure 2, B and C), at a time when obesity was established (Supplemental Figure 2A), while energy expenditure
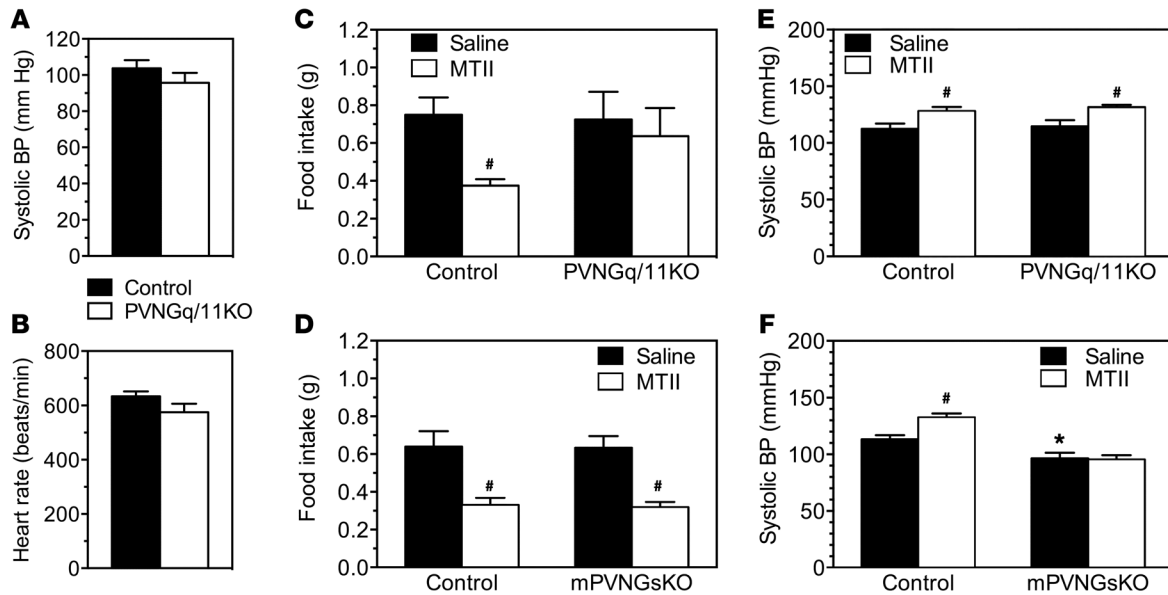
Figure 3. Differential effects of MTII injections in the PVNs of PVNGq/11KO and mPVNGsKO mice. (**A**) Systolic BP and (**B**) HR in male PVNGq/11KO and control mice at 8 to 10 weeks (*n* = 8 per group). (**C**) Food intake and (**E**) systolic BP after injection of saline or MTII into the PVNs of PVNGq/11KO and control mice (*n* = 5–8 per group). (**D**) Food intake and (**F**) systolic BP after injection of saline or MTII into the PVNs of mPVNGsKO and control mice (*n* = 5–6 per group). Data are expressed as mean ± SEM. *$P < 0.05$ vs. controls at baseline, #$P < 0.05$ vs saline by Student's *t* test.

and activity levels remained unaffected (Supplemental Figure 2, D and E). These effects on food intake and energy expenditure were similar to those observed in SIM1 mutant mice (5) but opposite to those observed in obese mBrGsKO mice (9).

Impaired anorectic response to melanocortin agonist in PVNGq/11KO mice. We next examined the acute effects of MTII on food intake and energy expenditure. Similar to SIM1 mutant mice (5) and opposite to that observed in mBrGsKO mice (9), PVNGq/11KO mice showed impaired ability to reduce food intake in response to MTII (Figure 2L), while the ability of MTII to stimulate TEE was maintained (Figure 2M).

MC3/4R activation of $G_s\alpha$ in the PVN has been shown to increase sympathetic nerve activity to the cardiovascular system and increase blood pressure (BP) and heart rate (HR) (21), and we recently confirmed this by showing that mPVNGsKO mice (also generated using *Sim1-Cre*) have reduced BP and HR (10). In contrast, BP and HR were unaffected in PVNGq/11KO mice (Figure 3, A and B), showing that even within the PVN distinct physiological effects of MC3/4R may be mediated through different G proteins.

To directly examine the effects of PVN-specific $G_s\alpha$ and $G_{q/11}\alpha$ deficiency on melanocortin-induced actions, cannulas were placed unilaterally in mPVNGsKO and PVNGq/11KO mice to allow direct delivery of MTII to the PVN, and its acute effects on food intake and systolic BP were examined. The dose of MTII was chosen based upon pilot experiments in control mice to determine the optimal dose for inhibition of food intake. In PVNGq/11KO mice, the ability of MTII injected into the PVN to inhibit food intake was lost in PVNGq/11KO mice (Figure 3C), while the ability of the same MTII injection to increase systolic BP was unaffected (Figure 3E). As we have shown previously (10), baseline systolic BP was lower than normal in mPVNGsKO mice

(Figure 3F). In mPVNGsKO mice, the ability of MTII injected into the PVN to inhibit food intake was unaffected (Figure 3D), while the ability of MTII to stimulate systolic BP was lost (Figure 3F). These experiments directly confirm that melanocortin actions on food intake and BP in the PVN are mediated via distinct G protein pathways and that inhibition of food intake by melanocortins in the PVN is mediated by $G_{q/11}\alpha$. The residual inhibition of food intake observed in response to i.p. MTII administration (Figure 2L) may represent the effects of the melanocortin agonist on peripheral sites (e.g., the gastrointestinal tract) (22) or other CNS sites (23, 24) or may be secondary to other metabolic changes resulting from systemic MTII administration.

Altered glucose and cholesterol metabolism in PVNGq/11KO mice. Older PVNGq/11KO mice developed hyperglycemia, hyperinsulinemia, glucose intolerance, and insulin resistance after becoming obese (24–28 weeks of age; Figure 4, C and D, and Table 1). However, glucose metabolism and insulin action were unaffected prior to the onset of obesity (6–8 weeks of age; Figure 4, A and B, and Table 1), in contrast to *Mc4r*−/− (1) and mBrGsKO mice (9), which have both been shown to develop glucose intolerance and insulin resistance at a young age, prior to the onset of obesity. This suggests that the primary effects of central melanocortins on glucose metabolism are mediated by $G_s\alpha$ rather than $G_{q/11}\alpha$.

Impaired melanocortin signaling has been shown to raise serum cholesterol levels (25). Serum cholesterol levels were significantly elevated in both young and old PVNGq/11KO mice (Table 1), while cholesterol levels were unaffected in 6- to 8-week-old mBrGsKO mice (mBrGsKO, 99 ± 10 mg/dl, vs. control, 91 ± 11 mg/dl, *n* = 5 per group). Serum-free fatty acid, triglyceride, and adiponectin levels were unaffected in PVNGq/11KO mice (Table 1). These results suggest that central melanocortin effects on cholesterol are mediated primarily by $G_{q/11}\alpha$ rather than $G_s\alpha$.
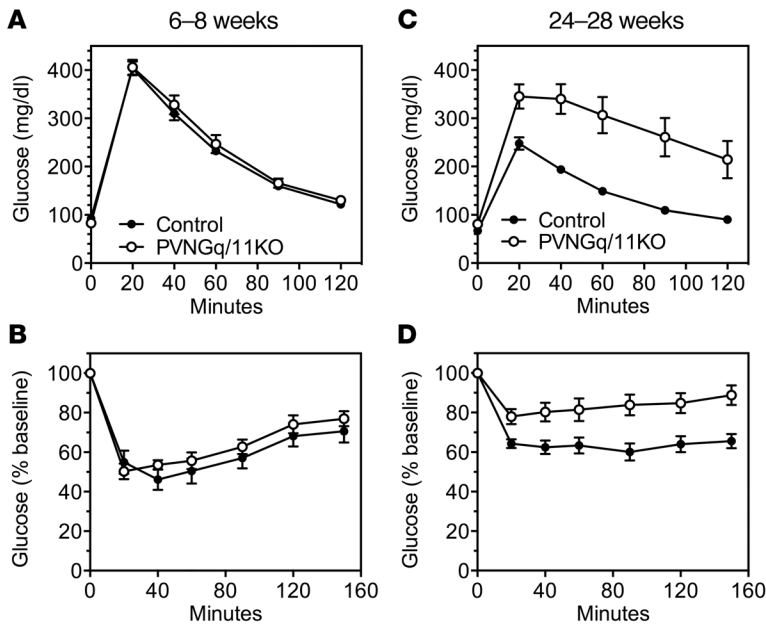
Figure 4. Glucose metabolism and cardiovascular function in PVNGq/11KO mice. (**A** and **C**) Glucose tolerance tests performed in (**A**) 6- to 8-week-old (n = 11–12 per group) and (**C**) 24- to 28-week-old female PVNGq/11KO and control mice (n = 9–10 per group). (**B** and **D**) Insulin tolerance tests performed in (**B**) 6- to 8-week-old (n = 7–10 per group) and (**D**) 24- to 28-week-old female PVNGq/11KO and control mice (n = 8–15 per group). AUCs for glucose and insulin tolerance tests were significantly different at 24 to 28 weeks ($P < 0.05$ by Student's t test) but not at 6 to 8 weeks. Data are expressed as mean ± SEM.

Altered gene expression in the PVNs of PVNGq/11KO mice. We next examined the expression of various genes in the PVN by qRT-PCR. In PVNGq/11KO mice, *Mc4r* gene expression was unaffected, while *Sim1* expression was significantly (26%) reduced (Figure 5A). Reduced *Sim1* expression may be a direct effect of loss of MC4R/$G_{q/11}\alpha$ signaling and may contribute to hyperphagic obesity and increased linear growth, as *Sim1* expression in the PVN has been shown to be induced by melanocortin signaling (5) and *Sim1* haploinsufficiency is sufficient to lead to hyperphagic obesity and increased linear growth (5, 7). In contrast, mPVNGsKO mice showed no loss of *Sim1* expression (Figure 5B), providing further evidence that regulation of *Sim1* by MC4R in the PVN is mediated by $G_{q/11}\alpha$ rather than $G_s\alpha$. Although it has been reported that SIM1 deficiency leads to hyperphagic obesity via reduction of oxytocin (*Oxt*) expression (26), *Oxt* expression in the PVNs of PVNGq/11KO mice was unaffected (Figure 5A), suggesting that other mechanisms downstream or independent of SIM1 may also be important in regulating food intake. Except for the gene encoding corticotropin-releasing hormone (*Crh*), which is discussed below, we observed no other changes in gene expression in the PVNs of PVNGq/11KO mice.

To directly answer whether MTII can stimulate *Sim1* and *Crh* gene expression and whether this action is mediated by $G_{q/11}\alpha$, expression of these genes in the PVN were examined 2 hours after i.p. administration of PBS or MTII (5 mg/kg). In this experiment, baseline (after PBS administration) *Sim1* and *Crh* mRNA levels were reduced by 40% and 48%, respectively, in PVNGq/11KO mice (Figure 5, C and D), confirming our original findings. MTII administration increased *Sim1* and *Crh* mRNA levels by 38% and 75%, respectively, in controls, while MTII had no effect in PVNGq/11KO mice (Figure 5, C and D). These results show that MC4R activation leads to induction of *Sim1* and *Crh* expression in a $G_{q/11}\alpha$-dependent manner. In contrast, *Oxt* gene expression was unaffected by MTII and was similar in control and PVNGq/11KO mice (Figure 5E).

Impaired hypothalamic-pituitary-adrenal axis in PVNGq/11KO mice. Expression of the *Crh* gene, another gene that is upregulated by MC4R activation (27), was significantly (30%) reduced in PVNGq/11KO mice but not in mPVNGsKO mice (Figure 5, A and B), indicating that CRH induction by melanocortins (and likely other factors) in the PVN is mediated by $G_{q/11}\alpha$. In line with reduced *Crh* expression, PVNGq/11KO mice had severe adrenal insufficiency, with markedly reduced serum adrenocorticotropin hormone (ACTH) and corticosterone levels (Figure 6), while we reported previously that corticosterone levels were unaffected in mBrGsKO mice (9). In addition, the stimulation of ACTH and corticosterone release at 1 hour after injection of insulin observed in control mice was significantly blunted in PVNGq/11KO mice (Figure 6), consistent with dysregulation of the hypothalamo-pituitary-adrenal axis at the level of the CNS.

AAV-Cre–mediated $G_{q/11}\alpha$ signaling deficiency in the PVN leads to hyperphagic obesity. As *Sim1* expression, which was used to drive Cre expression in PVNGq/11KO mice, is not limited to the PVN, we generated mice with $G_{q/11}\alpha$ deficiency specifically in the PVN by bilateral stereotaxic injection of adeno-associated virus–expressing Cre (AAV-Cre-GFP) into the PVNs of *Gnaq^{fl/fl} Gna11^{-/-}* mice to generate AAV-PVNGq/11KO mice. The same mice injected with AAV-GFP were used as controls. The injection sites were verified by fluorescence imaging (Figure 7A), and AAV-Cre-GFP injection led to an approximately 84% reduction in the PVN *Gnaq* mRNA (Figure 7B). By 10 weeks after injection, AAV-PVNGq/11KO mice developed severe obesity with a 2-fold increase in body weight relative to that of controls (Figure 7C), associated with significant hyperphagia (Figure 7D, 33% increase in food intake), which was measured at 4 weeks after injection (22% increase in body weight, data not shown). Similar to that in PVNGq/11KO mice, AAV-PVNGq/11KO mice also showed marked reductions in the PVN *Sim1* and *Crh* mRNA levels, with no change in *Mc4r* mRNA levels (Figure 7B). As a control, we also knocked out *Gnaq* and *Gna11* in the basomedial amygdala (BMA), another region in which *Sim1* is expressed, by bilateral stereotaxic injection of AAV-Cre-GFP into this region in *Gnaq^{fl/fl} Gna11^{-/-}* mice, which led to an 80% reduction in $G_q\alpha$ expression (Supplemental Figure 3, A and B). This manipulation produced no effect on either body weight or food intake (Supplemental Figure 3, C and D).
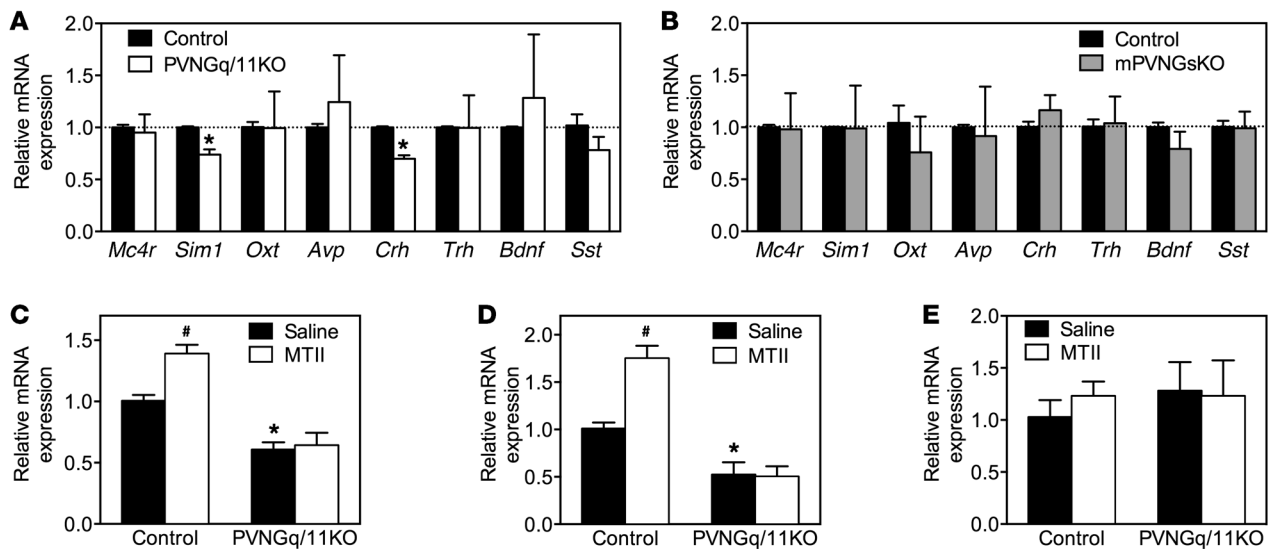
Discussion

While it has been recently established that MC4R-expressing neurons in the PVN (PVN^{MC4R}) primarily mediate their anorectic effect via excitatory (glutaminergic) inputs to the lateral parabrachial nucleus (28, 29), the signaling mechanisms by which MC4R activation leads to neuronal activation in these PVN neurons has not been established. MC4R is well known to couple to $G_s\alpha$. However, we have shown that $G_s\alpha$ deficiency in either the whole brain (9) or

Figure 5. Reduced *Sim1* and *Crh* expression in PVNGq/11KO mice. (**A** and **B**) PVN mRNA levels of various genes in (**A**) 8- to 10-week-old female PVNGq/11KO mice and (**B**) 12- to 16-week-old male mPVNGsKO mice and their littermate controls (n = 3–4 per group). *Avp*, arginine vasopressin; *Trh*, thyrotropin-releasing hormone; *Bdnf*, brain-derived neurotrophic factor; *Sst*, somatostatin. (**C**–**E**) Relative mRNA expression in the PVN of (**C**) *Sim1*, (**D**) *Crh*, and (**E**) *Oxt* 2 hours after administration of saline or MTII (5 mg/kg i.p.) in 8- to 10-week-old female control and PVNGq/11KO mice (n = 6 per group). Data are all normalized to controls and expressed as mean ± SEM. *$P < 0.05$ vs. controls, #$P < 0.05$ vs. saline by Student's t test corrected for repeated measures.

in the PVN (10) has no significant effect on food intake. Moreover, many MC4R mutations associated with human obesity do not alter MC4R signaling through $G_s\alpha$ (11), implicating an alternate signaling pathway. Although it has been recently shown that MC4Rs in PVN neurons can activate a inwardly rectifying potassium channel (Kir7.1) via a G protein–independent mechanism (30), the role of this pathway in regulation of food intake and the identification of the specific PVN^MC4R neuron population in which this pathway is operant has not been established. Studies have also established that MC4Rs are capable of activating Ca^{2+} signaling, presumably via $G_q\alpha$ and $G_{11}\alpha$, in cultured cell systems, including hypothalamic cells (15–17). We now show using an assay measuring IP_1 accumulation that a melanocortin MC3/4R agonist can induce PLC activity in the PVNs of control mice and that this effect requires $G_{q/11}\alpha$, as IP_1 induction by MTII is absent in PVNGq/11KO mice. Our results, however, do not fully rule out the possibility that PLC activation by MC4R occurs via an indirect mechanism rather than through direct activation of $G_{q/11}\alpha$.

In addition, we showed that loss of $G_q\alpha$ and $G_{11}\alpha$ in SIM1 neurons leads to hyperphagic obesity in PVNGq/11KO mice and confirmed that these effects on food intake and body weight result specifically from loss of $G_{q/11}\alpha$ in PVN neurons by direct injection of AAV-Cre-GFP into the PVNs of *Gnaq*^fl/fl *Gna11*^-/- mice. In contrast, similar injection of AAV-Cre-GFP into the BMA, another region containing SIM1 neurons, had no effect on energy balance. This coincides with recent studies confirming that MC4R actions on feeding in the CNS are primarily restricted to the PVN (28). We further established that $G_{q/11}\alpha$ mediates the regulation of food intake by MC4R in the PVN by showing that direct injection of MTII into the PVNs of PVNGq/11KO mice failed to elicit an anorectic effect, while the anorectic effect of MTII injection into the PVNs was maintained in mPVNGsKO mice. As a control, MTII injection into the

PVNs of PVNGq/11KO mice was still able to elicit a rise in BP, an action that was shown previously to be mediated via $G_s\alpha$ (10, 21), while the ability of MTII injection into the PVN to raise BP was lost in mPVNGsKO mice.

Evidence for an important role for MC4R-dependent PLC/ Ca^{2+} signaling in PVN neurons in feeding regulation has also been reported in mice with knockout of the K^+-dependent Na^+/Ca^{2+} exchanger NCKX4, which develop a hypophagic phenotype that is dependent upon MC4R/PLC/Ca^{2+} signaling in PVN neurons (17). The reduced expression of *Sim1* in the PVNs of PVNGq/11KO mice and the inability of *Sim1* to be stimulated by MTII, an effect that was observed by us and by others (5), provide evidence that SIM1, a a transcription factor in the PVN known to be involved in feeding behavior (6, 7), is a downstream target of melanocortin signaling that is mediated by $G_{q/11}\alpha$.

While we have not established whether the distinct actions of PVN MC4R/$G_{q/11}\alpha$ signaling on feeding behavior and PVN MC4R/$G_s\alpha$ actions on cardiovascular function are occurring within the same cell or in different cell populations, it is more likely the latter, as it has been shown that PVN^MC4R neurons involved in feeding regulation project directly to the lateral parabrachial nucleus, with no other collateralization (29). Likewise, it is also unknown whether the effects resulting from loss of PVN $G_{q/11}\alpha$ that we observed on food intake versus linear growth or cholesterol metabolism are occurring in the same cell or in distinct neuron populations. PVN^MC4R neurons that regulate feeding are within a subset of NOS1-expressing neurons (31) that are distinct from *Oxt*-expressing neurons (28, 29, 31). These findings, as well as other evidence (32), suggest that *Oxt*-expressing neurons in the PVN do not play a significant role in the regulation of food intake, while other studies implicate these neurons in regulation of food intake (33). Our observations that *Oxt* expression in the PVN was unaffected in PVNGq/11KO mice, despite
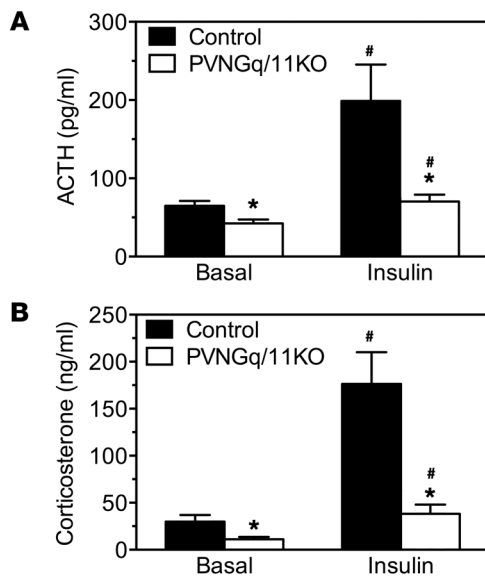
Figure 6. Impaired hypothalamic-pituitary-adrenal axis in PVNGq/11KO mice. (**A**) Serum ACTH and (**B**) corticosterone levels in female 16- to 20-week-old PVNGq/11KO mice at baseline (0900, fed) and 1 hour after insulin administration (0.75 mIU/g, i.p.). Data are expressed as mean ± SEM (*n* = 5–8 per group). *$P < 0.05$ vs. controls, #$P < 0.05$ vs. basal by Student's *t* test.

a clear hyperphagic phenotype, and that MTII administration did not affect *Oxt* expression in control mice are more consistent with *Oxt* probably not playing a major role in regulation of food intake by melanocortins. Further studies will be required to delineate the specific neuronal populations within the PVN in which MC4R/$G_{q/11}\alpha$ plays an important role.

We have also observed that loss of $G_{q/11}\alpha$ in the PVN leads to significantly reduced PVN *Crh* mRNA expression, impaired activation of the hypothalamic-pituitary-adrenal axis, and adrenal insufficiency. We directly confirmed in control mice that MTII administration leads to induction of *Crh* expression and that this induction is absent in PVNGq/11KO mice. It is unlikely that CRH deficiency contributes to obesity in PVNGq/11KO mice, as CRHKO mice have normal food intake and body size (34, 35), and recent studies suggest that CRH-expressing neurons in the PVN are not involved in feeding behavior (28, 29). Other GPCRs in addition to MC4R may also couple to $G_{q/11}\alpha$ and be important in regulating *Crh* expression in the PVN, as corticosterone levels have been reported to be unaffected in *Mc4r*^{-/-} mice (3).

In summary, MC4R activation mediates its diverse physiological effects via different pathways either within the same or in different CNS regions. The results of our prior and present studies indicate that, within the PVN, MC4R effects on food intake, linear growth, cholesterol metabolism, and *Sim1* and *Crh* gene expression are mediated by $G_{q/11}\alpha$, while MC4R effects on HR and BP are mediated via $G_s\alpha$ (Supplemental Figure 4) (9, 10). Outside of the PVN, MC4R mediates its effects on energy expenditure and glucose metabolism via $G_s\alpha$. Although we focused on MC4R, disruption of other GPCR/$G_{q/11}\alpha$ pathways in the PVN (and other *Sim1-Cre*–expressing sites) is also likely to contribute to the effects observed in PVNGq/11KO mice. For example, bombesin receptor subtype 3 is expressed in the PVN, couples to $G_{q/11}\alpha$, suppresses food intake,

and may control *Crh* expression (36, 37). The PVNGq/11KO model will be very useful to explore the role of other $G_{q/11}\alpha$-mediated pathways in metabolic regulation and neuroendocrine function. We believe that our findings identify a new potential therapeutic target for obesity, as a biased MC4R agonist that activates $G_{q/11}\alpha$ but not $G_s\alpha$ has the potential to suppress appetite, without the untoward cardiovascular effects observed with nonselective agonists (38).

Methods

Mice. Gnaq floxed mice (39) were crossed to the *Gna11*^{-/-} (14) and *Sim1-Cre* mice (4) to generate PVNGq/11KO mice (*Sim1-Cre Gnaq*^{fl/fl} *Gna11*^{-/-} mice). *Gnaq*^{fl/fl} *Gna11*^{-/-} littermates were used as controls, as we showed that these mice had no metabolic phenotype (Supplemental Figure 2). mPVNGsKO mice were generated by mating *Sim1-Cre* and maternal *Gnas*^{fl/-} mice as previously described (10). All mice were backcrossed onto a C57BL/6J background for 6 generations. Animals were maintained on a 12-hour-light/12-hour-dark cycle (with light from 0600 hours to 1800 hours) and standard pellet diet (NIH07, 5% fat by weight).

In situ hybridization. In situ hybridization of coronal brain slices was performed as previously described (9) using sense and antisense mRNA probes for *Gnas*, *Gnaq*, and *Gna11* (probe sequences for *Gnas*, *Gnaq*, and *Gna11* are shown in Supplemental Table 2). After hybridization, slices were exposed to NTB2 emulsion for 3 to 10 days and then counterstained with hematoxylin and eosin. Signals were quantified in dark-field images with Image-Pro Plus software (Media Cybernetics).

IP$_1$ determination. Mice were sacrificed, and PVNs were quickly collected and incubated in DMEM containing 4.5 g/l D-glucose (Gibco), 1% BSA (fatty acid–free, Sigma-Aldrich), and 50 mM LiCl for 2 hours at 37°C. PBS or MTII (50 nM final concentration) was then added and incubated for another 1 hour before the tissues were homogenized for the IP$_1$ assay (Cisbio Bioassays). Data were normalized to protein content (BCA Protein Assay, Thermo Scientific).

Food intake, body composition, and metabolic studies. Body composition was measured with the Echo3-in1 NMR analyzer (Echo Medical Systems). To measure food intake, mice were pair caged and allowed to acclimate for 1 week prior to measurement of food intake during the subsequent 2 weeks. O$_2$ consumption was measured at 24°C and 30°C, each over a 24-hour period in a CLAMS system (Columbus Instruments, 2.5-l chambers with plastic floors, using 0.6 l/min flow rate, 1 mouse per chamber). Motor activity (total and ambulatory) was simultaneously measured by infrared beam interruption. Resting O$_2$ consumption was calculated as the mean of the points with less than 6 ambulating beam breaks per minute. Prior to these studies, mice were acclimated for 1 day in the metabolic chamber at room temperature.

MTII injections. Mice were caged singly and acclimated with 3 daily i.p. injections of PBS. To study the effects on food intake, mice received MTII (5 mg/kg, i.p.) or PBS (200 μl) on separate days 30 minutes before lights out, and food intake was measured for 3.5 hours in the dark. For energy expenditure, mice were placed in indirect calorimetry chambers for 24 hours at 30°C. On the following day, while still maintained at 30°C, mice received either MTII (10 mg/kg, i.p.) or PBS at 1200 hours (12 PM). Total O$_2$ consumption was measured at between 1300 and 1500 hours (1 to 3 PM).

Glucose and insulin tolerance tests. For glucose tolerance tests, overnight-fasted mice received glucose (2 g/kg i.p.), and glucose was measured in blood drawn from tail veins at indicated time points
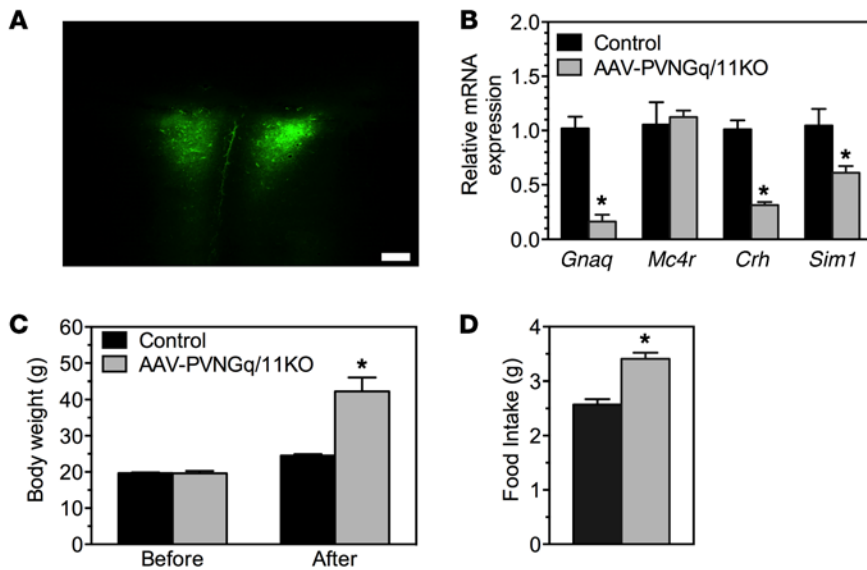
Figure 7. AAV-PVNGq/11KO mice are hyperphagic and obese. (A) Representative image (original magnification, ×10; scale bar: 200 μM) showing fluorescence localized to PVN at 10 weeks after bilateral injection of AAV-Cre-GFP. **(B)** PVN mRNA levels of $G_q\alpha$ (*Gnaq*), *Mc4r*, *Crh*, and *Sim1* measured 10 weeks after viral injection in AAV-PVNGq/11KO and control mice (*n* = 4 per group). **(C)** Body weight of AAV-PVNGq/11KO and control mice measured before and 10 weeks after viral injection (*n* = 6 per group). **(D)** Daily food intake of AAV-PVNGq/11KO and control mice measured 4 weeks after viral injection (*n* = 6 per group). Data are expressed as mean ± SEM. *P < 0.05 vs. controls by Student's *t* test.

with a glucometer (Contour, Bayer). For insulin tolerance tests, mice were fasted for 5 hours prior to administration of insulin (Humulin, 0.75 mIU/g, i.p.; Eli Lilly).

Serum chemistries. Glucose was measured with a glucometer (Contour, Bayer). Triglycerides were measured with Triglyceride (GPO) Liquid Reagent (Pointe Scientific). Free fatty acids were measured with the Half Micro Test (Roche). Total cholesterol was measured with Infinity Cholesterol Reagent (Thermo Scientific). Insulin, leptin, and adiponectin were measured using radioimmunoassay kits (Sensitive Rat Insulin RIA Kit, Mouse Leptin RIA Kit, and Mouse Adiponectin RIA Kit, respectively; Millipore). ACTH and corticosterone were measured by ELISA with kits obtained from MD Bioproducts and Enzo Life Science, respectively.

Microdissection and real-time quantitative RT-PCR. Mice were anesthetized and sacrificed by decapitation, and brains were immediately flash frozen on dry ice. PVN and MBA were collected by micropunching of brain slices (100 μm) from bregma −0.56 mm to −0.96 mm for PVN and bregma −0.94 to −1.34 for MBA (35). Total RNA was extracted using NucleoSpin RNA XS (Clontech) and treated with DNAse I (Invitrogen) at room temperature for 15 minutes. Reverse transcription was performed using MultiScribe RT (Applied Biosystems). Gene expression levels were measured by real-time quantitative RT-PCR (MxP3000; Stratagene). PCR reactions included cDNA (20–40 ng of initial RNA sample), 50–100 nM primers, and 10 μl of 2× SYBR Green Master Mix (Roche) and were performed in a total volume of 20 μl. Standard curves were simultaneously generated with serial dilutions of cDNA, ranging from 1 to 100 ng, and results were normalized to β-actin mRNA levels in each sample, which were determined simultaneously by the same method. Specificity of each RT-PCR product was checked by its dissociation curve and the presence of a single band of the expected size on acrylamide gel electrophoresis. Primer sequences are provided in Supplemental Table 1.

BP and HR measurements. Systolic BP and HR were measured with a BP-2000 Specimen platform (Visitech). Prior to measurement, mice were acclimated by being placed in the apparatus daily for 7 days.

Stereotaxic microinjection of AAV. 6- to 8-week-old female *Gnaq^{fl/fl}* *Gna11^{−/−}* mice were bilaterally injected with 50 nl of either AAV2-CMV-PI-eGFP-WPRE-bGH (AAV-GFP; 6.92 × 10^{12} genomic copies/ml)

or AAV2-CMV-HI-GFP-CRE-WPRE-SV40 (AAV-Cre-GFP; 5.5 × 10^{12} genomic copies/ml) (catalog AV-2-PV0101 and catalog AV-2-PV-2004, respectively, Penn Vector Core) into the PVN (bregma: anterioposterior, −0.82 mm; mediolateral, ±0.2 mm; dorsoventral, −4.8 mm), using a stereotaxic apparatus. Similarly, 100 nl of either AAV was bilaterally injected into the BMA (bregma: anterioposterior, −0.9 mm; mediolateral, ±2.3 mm; dorsoventral, −5.37 mm) in separate sets of *Gnaq^{fl/fl}* *Gna11^{−/−}* mice. Surgery was performed under isoflurane anesthesia (5% induction, 1.5%–2.5% maintenance via inhalation), and body temperature was maintained at 37°C throughout the procedure. Topical lidocaine (0.1 ml of 2% solution) was injected along the midline of the scalp before an incision was made to access the skull. Two burr holes were drilled at the bilateral coordinates, as mentioned above, using a drill (model 1474, David Kopf Instruments). Infusions were made via pulled borosilicate glass micropipette with a tip outer diameter of 30 to 50 μm. The micropipette was connected to a pneumatic pump (Picospritzer III, Parker Hannifin Precision Fluidics Division), and the AAVs were infused with short air puffs (each puff, 5 ms) at 10 to 20 psi until the 50-nl volume was infused. Infusions were made over a period of 10 minutes, and the micropipette was left in place for 5 minutes to prevent backflow. After withdrawing the pipette slowly out of the injection site, skull holes were sealed with bone wax and incisions were closed with 7-mm wound clips (Roboz Surgical Instruments Co. Inc). Mice were injected with Banamine (2.2 mg/kg s.c.) to reduce inflammation.

PVN injections of MTII. 6- to 8-week-old female PVNGq/11KO and mPVNGsKO mice and their respective littermate controls were implanted with sterile unilateral 26-gauge stainless steel guide cannulas on their right sides (coordinates 0.2 mm lateral, 0.82 mm posterior to the bregma, and 4.13 mm below the skull) and anchored with the help of jeweler's screws, cyanoacrylate, and dental cement (Plastics One). Incisions were closed, and a dummy cap was screwed onto the cannula to prevent from contamination or blockage. One week after surgery, mice were acclimated to handling and injections with PBS for 3 consecutive days before testing the effect of MTII on either food intake or BP. To study effects on food intake, 200 nl MTII (33 pmol) or PBS was injected into the PVN via an internal cannula connected to a 10-μl syringe with PE tubing that extended 0.5

mm below the tip of the guide cannula 1 hour before lights out, and food intake was measured for 3.5 hours in the dark. The same set of mice was tested for MTII's effect on BP after 1 week of acclimation to the procedure; the same volume and dosage of MTII or PBS used in food intake study was injected into the PVN 2 hours before systolic BP was measured.

Statistics. All data are expressed as mean ± SEM and were analyzed by 2-tailed Student's *t* test or 1-way ANOVA using Prism 4 (GraphPad), with differences considered significant at $P < 0.05$.

Study approval. All animal studies were approved by the Animal Care and Use Committee of the NIDDK.

Author contributions

YQL, YS, and LSW designed the research study and experiments. YQL, YS, MP, MC, AK, and OG conducted experiments and acquired and analyzed data. SO provided the *Gna11⁻/⁻* and *Gnaq⁻/⁻* mice. YQL and LSW wrote the manuscript. All authors read and commented on the manuscript.

1. Fan W, Dinulescu DM, Butler AA, Zhou J, Marks DL, Cone RD. The central melanocortin system can directly regulate serum insulin levels. *Endocrinology.* 2000;141(9):3072–3079.
2. Farooqi IS, Keogh JM, Yeo GS, Lank EJ, Cheetham T, O'Rahilly S. Clinical spectrum of obesity and mutations in the melanocortin 4 receptor gene. *N Engl J Med.* 2003;348(12):1085–1095.
3. Huszar D, et al. Targeted disruption of the melanocortin-4 receptor results in obesity in mice. *Cell.* 1997;88(1):131–141.
4. Balthasar N, et al. Divergence of melanocortin pathways in the control of food intake and energy expenditure. *Cell.* 2005;123(3):493–505.
5. Kublaoui BM, Holder JL Jr, Gemelli T, Zinn AR. Sim1 haploinsufficiency impairs melanocortin-mediated anorexia and activation of paraventricular nucleus neurons. *Mol Endocrinol.* 2006;20(10):2483–2492.
6. Kublaoui BM, Holder JL Jr, Tolson KP, Gemelli T, Zinn AR. SIM1 overexpression partially rescues agouti yellow and diet-induced obesity by normalizing food intake. *Endocrinology.* 2006;147(10):4542–4549.
7. Holder JL Jr, Butte NF, Zinn AR. Profound obesity associated with a balanced translocation that disrupts the SIM1 gene. *Hum Mol Genet.* 2000;9(1):101–108.
8. Weinstein LS, Xie T, Qasem A, Wang J, Chen M. The role of GNAS and other imprinted genes in the development of obesity. *Int J Obes (Lond).* 2010;34(1):6–17.
9. Chen M, et al. Central nervous system imprinting of the G protein G$_s$α and its role in metabolic regulation. *Cell Metab.* 2009;9(6):548–555.
10. Chen M, Berger A, Kablan A, Zhang J, Gavrilova O, Weinstein LS. G$_s$α deficiency in the paraventricular nucleus of the hypothalamus partially contributes to obesity associated with Gsα mutations. *Endocrinology.* 2012;153(9):4256–4265.
11. Hinney A, et al. Melanocortin-4 receptor gene: case-control study and transmission disequilibrium test confirm that functionally relevant mutations are compatible with a major gene effect for extreme obesity. *J Clin Endocrinol Metab.* 2003;88(9):4258–4267.
12. Maudsley S, Martin B, Luttrell LM. The origins

of diversity and specificity in G protein-coupled receptor signaling. *J Pharmacol Exp Therap.* 2005;314(2):485–494.
13. Offermanns S, et al. Impaired motor coordination and persistent multiple climbing fiber innervation of cerebellar Purkinje cells in mice lacking Gαq. *Proc Natl Acad Sci U S A.* 1997;94(25):14089–14094.
14. Offermanns S, Zhao LP, Gohla A, Sarosi I, Simon MI, Wilkie TM. Embryonic cardiomyocyte hypoplasia and craniofacial defects in Gαq/Gα11-mutant mice. *EMBO J.* 1998;17(15):4304–4312.
15. Newman EA, Chai BX, Zhang W, Li JY, Ammori JB, Mulholland MW. Activation of the melanocortin-4 receptor mobilizes intracellular free calcium in immortalized hypothalamic neurons. *J Surg Res.* 2006;132(2):201–207.
16. Peters MF, Scott CW. Evaluating cellular impedance assays for detection of GPCR pleiotropic signaling and functional selectivity. *J Biomolec Screening.* 2009;14(3):246–255.
17. Li XF, Lytton J. An essential role for the K⁺-dependent Na⁺/Ca²⁺-exchanger, NCKX4, in melanocortin-4-receptor-dependent satiety. *J Biol Chem.* 2014;289(37):25445–25459.
18. Jin LQ, Wang HY, Friedman E. Stimulated D1 dopamine receptors couple to multiple Gα proteins in different brain regions. *J Neurochem.* 2001;78(5):981–990.
19. Boutin A, Allen MD, Neumann S, Gershengorn MC. Persistent signaling by thyrotropin-releasing hormone receptors correlates with G-protein and receptor levels. *FASEB J.* 2012;26(8):3473–3482.
20. Holder JL Jr, et al. Sim1 gene dosage modulates the homeostatic feeding response to increased dietary fat in mice. *Am J Physiol Endocrinol Metab.* 2004;287(1):E105–E113.
21. Li P, Cui BP, Zhang LL, Sun HJ, Liu TY, Zhu GQ. Melanocortin 3/4 receptors in paraventricular nucleus modulate sympathetic outflow and blood pressure. *Exp Physiol.* 2013;98(2):435–443.
22. Panaro BL, et al. The melanocortin-4 receptor is expressed in enteroendocrine L cells and regulates the release of peptide YY and glucagon-like peptide 1 in vivo. *Cell Metab.*

2014;20(6):1018–1029.
23. Grill HJ, Ginsberg AB, Seeley RJ, Kaplan JM. Brainstem application of melanocortin receptor ligands produces long-lasting effects on feeding and body weight. *J Neurosci.* 1998;18(23):10128–10135.
24. Williams DL, Kaplan JM, Grill HJ. The role of the dorsal vagal complex and the vagus nerve in feeding effects of melanocortin-3/4 receptor stimulation. *Endocrinology.* 2000;141(4):1332–1337.
25. Perez-Tilve D, et al. Melanocortin signaling in the CNS directly regulates circulating cholesterol. *Nat Neurosci.* 2010;13(7):877–882.
26. Kublaoui BM, Gemelli T, Tolson KP, Wang Y, Zinn AR. Oxytocin deficiency mediates hyperphagic obesity of Sim1 haploinsufficient mice. *Mol Endocrinol.* 2008;22(7):1723–1734.
27. Lu XY, Barsh GS, Akil H, Watson SJ. Interaction between α-melanocyte-stimulating hormone and corticotropin-releasing hormone in the regulation of feeding and hypothalamo-pituitary-adrenal responses. *J Neurosci.* 2003;23(21):7863–7872.
28. Shah BP, et al. MC4R-expressing glutamatergic neurons in the paraventricular hypothalamus regulate feeding and are synaptically connected to the parabrachial nucleus. *Proc Natl Acad Sci U S A.* 2014;111(36):13193–13198.
29. Garfield AS, et al. A neural basis for melanocortin-4 receptor-regulated appetite. *Nat Neurosci.* 2015;18(6):863–871.
30. Ghamari-Langroudi M, et al. G-protein-independent coupling of MC4R to Kir7.1 in hypothalamic neurons. *Nature.* 2015;520(7545):94–98.
31. Sutton AK, Pei H, Burnett KH, Myers MG Jr, Rhodes CJ, Olson DP. Control of food intake and energy expenditure by Nos1 neurons of the paraventricular hypothalamus. *J Neurosci.* 2014;34(46):15306–15318.
32. Wu Z, et al. An obligate role of oxytocin neurons in diet induced energy expenditure. *PLoS One.* 2012;7(9):e45167.
33. Atasoy D, Betley JN, Su HH, Sternson SM. Deconstruction of a neural circuit for hunger. *Nature.* 2012;488(7410):172–177.
34. Jacobson L. Glucocorticoid replacement, but not corticotropin-releasing hormone deficiency, pre-

vents adrenalectomy-induced anorexia in mice. *Endocrinology*. 1999;140(1):310–317.

35. Muglia L, Jacobson L, Dikkes P, Majzoub JA. Corticotropin-releasing hormone deficiency reveals major fetal but not adult glucocorticoid need. *Nature*. 1995;373(6513):427–432.

36. Zhang L, Parks GS, Wang Z, Wang L, Lew M, Civelli O. Anatomical characterization of bomb-esin receptor subtype-3 mRNA expression in the rodent central nervous system. *J Comp Neurol*. 2013;521(5):1020–1039.

37. Jensen RT, Battey JF, Spindel ER, Benya RV. International Union of Pharmacology. LXVIII. Mammalian bombesin receptors: nomenclature, distribution, pharmacology, signaling, and functions in normal and disease states. *Pharmacol Rev*. 2008;60(1):1–42.

38. Greenfield JR. Melanocortin signalling and the regulation of blood pressure in human obesity. *J Neuroendocrinol*. 2011;23(2):186–193.

39. Wettschureck N, et al. Absence of pressure overload induced myocardial hypertrophy after conditional inactivation of Gαq/Gα11 in cardiomyocytes. *Nat Med*. 2001;7(11):1236–1240.